

NATIONAL AIR INTELLIGENCE CENTER



PHOTO-REFRACTIVE $\text{Bi}_{12}\text{SiO}_{20}$ - SPATIAL LIGHT MODULATOR

by

Mingjun Zhao, Yulin Li, Zhao Wang



19950407 094

Approved for public release;
Distribution unlimited.

DTIC QUALITY INSPECTED 5



HUMAN TRANSLATION

NAIC-ID(RS)T-0396-94

27 March 1995

MICROFICHE NR: 95 C000 113

PHOTO-REFRACTIVE Bi₁₂SiO₂₀ - SPATIAL LIGHT MODULATOR

By: Mingjun Zhao, Yulin Li, Zhao Wang

English pages: 9

Source: Guangxue Xuebao, Vol. 11, Nr. 9, September 1991;
pp. 810-814

Country of origin: China

Translated by: SCITRAN
F33657-84-D-0165

Requester: NAIC/TATA/J.M. Finley
Approved for public release; Distribution unlimited.

Accession For	
NTIS CRA&I	<input checked="" type="checkbox"/>
DTIC TAB	<input type="checkbox"/>
Unannounced	<input type="checkbox"/>
Justification _____	
By _____	
Distribution / _____	
Availability Codes	
Dist	Avail and/or Special
A-1	

THIS TRANSLATION IS A RENDITION OF THE ORIGINAL FOREIGN TEXT WITHOUT ANY ANALYTICAL OR EDITORIAL COMMENT STATEMENTS OR THEORIES ADVOCATED OR IMPLIED ARE THOSE OF THE SOURCE AND DO NOT NECESSARILY REFLECT THE POSITION OR OPINION OF THE NATIONAL AIR INTELLIGENCE CENTER.	PREPARED BY: TRANSLATION SERVICES NATIONAL AIR INTELLIGENCE CENTER WPAFB, OHIO
--	---

GRAPHICS DISCLAIMER

All figures, graphics, tables, equations, etc. merged into this translation were extracted from the best quality copy available.

Abstract

This paper uses non-degenerate and degenerate multi-wave mixing frequencies of the photo-refractive $\text{Bi}_{12}\text{SiO}_{20}$ crystal to create incoherent - coherent conversions; wavelength conversion and image subtraction between coherent and incoherent images, and thus experimental results are so given.

Keywords: Photo-refractive crystal, 4-wave mixing frequencies

1. INTRODUCTION

The device or equipment which can amplify optical spatial information, polarize the amplitudes, modulate phases or wavelengths, etc. is generally called a spatial light modulator. Such operation is determined by the location where such distributed optical information is found, and thus it is called as an optical searching locality spatial light modulator. In the optical information processing and optical computing system, one can utilize the fast speed of light, to carry out processing and high grade mutual correlative capability. Thus it receives

* Numbers in margins indicate foreign pagination.
Commas in numbers indicate decimals.

¹ Subject of the National Natural Science Funds' Support.

² Xian Institute of Optics and Precision Mechanics, Academia Sinica Xian 710068.

Date of receiving: November 8, 1990; Date of receiving the revised version: February 5, 1991

ever more attention from researchers. At present, the widely used spatial light modulating devices are liquid crystal optical valve, variable reflective mirror, micro-channel spatial light modulating devices, semiconducting multi-quantum potential well, magnetic light, etc. [1-2]. In utilizing photo-refractive crystal $\text{Bi}_{12}\text{SiO}_{20}$ (BSO) as a spatial light modulating device, to begin with there was PROM device (Pockels readout optical modulator) [3] but soon afterwards based on the study on photo-refractive nonlinearity, Shi et al. [4] proposed that using degenerate 4-wave mixing frequencies of a photo-refractive crystal and adding incoherent light modulation one can realize the conversion of incoherent images to coherent image; that is, it is none other than a PICOC (a Photo-refractive incoherent-to-coherent optical converter). This adds some new features to the research and application efforts of spatial light modulators [5].

This paper is intended to make a report on the author's experimental research on the home-made BSO crystal refractive characteristics [6] as the starting point, first to utilize its degenerate and non-degenerate multi-wave mixing frequencies in realizing incoherent-coherent image conversion, and to go one-step further in utilizing such systems to complete image-storage; wavelength conversion; carrying out the subtraction operation on coherent and incoherent image and thus to provide the experimental results herewith.

2. PHOTO-REFRACTIVE EFFECT AND 4-WAVE MIXING FREQUENCIES

Fig.1 is the schematic diagram of 4-wave mixing frequencies of photo-refractive crystal, in which the incident wave E_1 and signal wave E_3 create a periodic

optical intensity distribution inside the photo-refractive crystal, the irradiation creates the transmission (dissipation and floating) of optical carrier flows from the bright spot to the shaded spot, and afterwards builds up a spatial electric charge field:

$$E_{sc} = E_q \left[\frac{E_a^2 + E_d^2}{E_a^2 + (E_d + E_q)^2} \right]^{1/2}, \quad (1)$$

where E_q is the maximum electric charge field; E_d is dissipation field; E_a is an externally added electric field. The periodic electric field passes through an electrophoto effect to modulate crystalline refractive index in creating a periodic distribution,

$$\Delta n = (1/2)n_b^3 r_{eff} E_{sc} \quad (2)$$

where n_b is the refractive index of the crystal; r_{eff} is the effective electric-photo effect coefficient. The process of its photo-refractive effect is as shown in Fig. 2.

If one uses the reference wave E_2 which is a reverse of E_1 to read out the waves, then one obtains the conjugate wave E_4 which is the reverse of E_3 . Thus the so-called 4-wave mixing frequencies system is constructed.

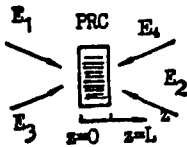


Fig. 1 Schematic diagram of photo-refractive four-wave mixing

If in Eqn.(1) $E_a > E_d$, and also $E_q > E_a$, then the externally added electric field has a leading role, namely $E_{sc} \propto E_c$. Thus the externally added electric field and the refractive index form a direct proportionality, but for

further discussions on the phase conjugation of the photo-refractive BSO crystal and the diffractive effect of its body holographic grating, one may refer to Ref.[6].

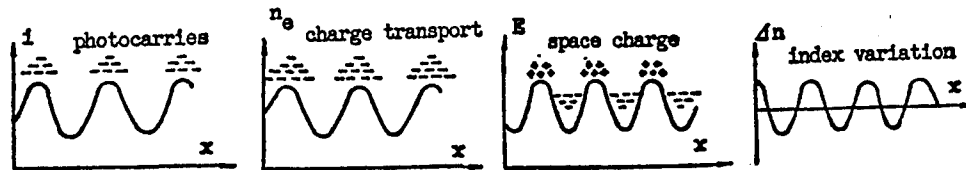


Fig. 2 Photorefractive effect process

The BSO crystal belongs to a cubic crystal, of point-group 23, possessing both a prominent electro-photo effect as well as photoelectric effect and its response time is faster than those of BaTiO₃ and LiNbO₃ crystals by 3 orders of magnitude [7 - 8]. Fig. 3 shows the working principles' diagram of how the photo-refractive BSO (10 x 10 x 3 mm³) multiwave mixing frequencies carry out the incoherent-coherent conversion, and moreover it shows that the added electric field (along the 001-axis) and the optical grating vector are parallel. If E₁ and E₃ incoherent light or white light are being used to form images at the crystal, then incoherent light would carry out spatial modulation to the optic gratings which have been created by E₁ and E₃; the results of modulation would transport the information, carried along by the incoherent light to the spatial grating so that at the time coherent reference wave E₂ can read out the optic grating, and then the 4th conjugate output wave E₄ brings with it the incoherent information. In this way the conversion from incoherent images to coherent images is completed.

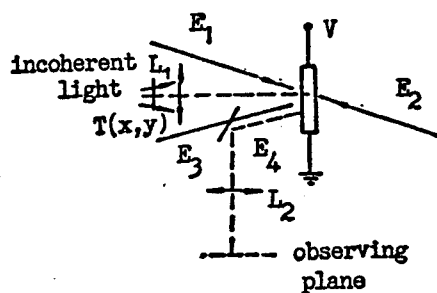


Fig. 3 Experimental setup for PICOC in FWM with BSO crystal

In the experiment made for this paper, the 4-wave mixing frequencies used the Ar^+ laser beam as the coherent light source ($\lambda = 514.5 \text{ nm}$), while the incoherent images used white flaming light to pass through lens L_1 ($f_1 = 22 \text{ cm}$; $\phi = 5 \text{ cm}$) of BSO crystal, applying a high voltage field $E_a = 8 \text{ kV}\cdot\text{cm}^{-1}$ to the crystal to get the results of one complete conversion as shown in Fig. 4.

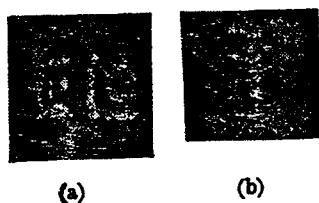


Fig. 4 The results of PICOC operation
(a) input an incoherent image; (b) output a negative replica of the input image

Fig.5(a) is to show how nondegenerate multiwave mixing frequencies complete a PICOC operation; that is, I_1 and I_2 from an Ar^+ laser device (514.5 nm) act on an external field so that they can construct a 3-dimensional optical grating inside BSO, then another flux from the He-Ne laser (632.8 nm) which satisfies the Bragg condition is emitted to BSO, to diffract out the 4th flux ray, called the He-Ne beam. If I_1 and I_2 contain the spatial information; or it lets other incoherent information be modulated to reach the optic grating; that is, it can transmit the diffracted He-Ne

beams, as shown in Fig. 5(b), in which $T(x,y)$ is the incoherent information; in Fig.5(a), $T(x,y)$ is the spatial image information of I_2 .

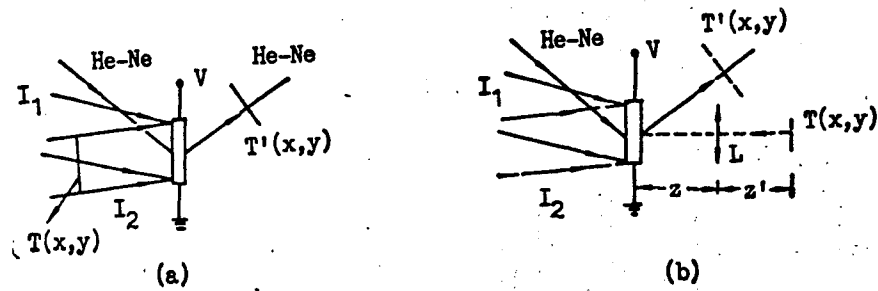


Fig. 5 PICOC is performed by using real-time holography
 (a) Green image (514.5 nm) was stored, it can be readout by red light (632.8 nm); (b) White image was stored, it can be readout by red (632.8 nm) or green (514.5 nm) light

3. EXAMPLES TO SHOW HOW IMAGES ARE PROCESSED

There have been quite a few reports made on the application of multiwave mixing frequencies of photo-refractive BSO crystal to complete image-processing [9-10], but they are all concerned with pure coherent computations, and here the present authors, based on the previously mentioned theories, want to apply them to image processing, including incoherent as well as coherent images, even including the contents involving optical computation operations, etc.

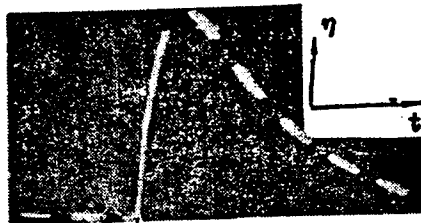


Fig. 6 The curve of diffraction efficiency dependence time for grating build up and decay in BSO ($10 \times 10 \times 3 \text{ mm}^3$; $E_s = 6 \text{ kV} \cdot \text{cm}^{-1}$) crystal [6]

1. Image Storage and Wavelength Conversion

Because a BSO crystal has the capability of real-time recording and storage, but more importantly under the added external electric field, the speed of constructing an optical grating picks up while the deteriorating process slows down [6], as shown in Fig. 6; when I_1 and I_2 are shone onto the crystal and on top of that white light images gather on the crystal but the time generally takes a bit longer (0.1 - 1 sec), because this mainly depends on the intensity of the white light; that is, the light is more intense, the shorter becomes the exposure. At this time one can cut off the Ar^+ beam so that the incoherent image information will be frozen inside the crystal. After a few minutes to few tens of minutes, if the plane waves of the He-Ne beam or the Ar^+ flux (I_1 or I_2) are used to read the optical grating, then one can get a coherent red or green light image. This is nothing but to complete an image conversion, as shown in Fig.7, in which white light is converted to red light ($\lambda = 632.8$ nm) or green light ($\lambda = 514.5$ nm) in a wavelength image conversion. Now in the process for I_1 and I_2 to construct the optical grating, due to the local responding characteristics of the BSO crystal, if I_1 or I_2 itself contains spatial information, namely placing a transparent object in the optical path of I_1 or I_2 , then using the He-Ne beam to make out an optical readout, one can obtain the corresponding spatial image, as shown in Fig. 8, and thus one completes the wavelength conversion³ of images in which green light ($\lambda = 514.5$ nm) is converted to red light ($\lambda = 632.8$ nm).

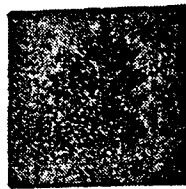
³ Here the complete conversion is a positive image conversion.

2. Incoherent and coherent image carrying out mutual attenuating operations

In the above incoherent to coherent image conversion process, the results of operations all showed negative images of the white light picture-images, but this is due to the reason that the white light picture-image prints itself inversely in order to cope with the erasing action of the optical grating, and thus the operation from the printing of the white picture-image to making a read-out corresponds to the completing of a "negative" operation. But coherent beam I_1 (or I_2) is a positive printing-down. If one provides picture-images for one of the coherent beams (I_1 or I_2) as well as for an incoherent one to carry them, a realization of a subtraction operation for these 2 is accomplished; the results of this operation can be read out by use of a He-Ne beam, as shown in Fig.9. Similarly one can apply such methods as the center piece of any optical logic computation operation.



(a)



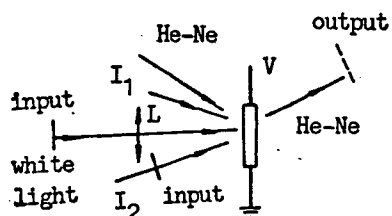
(b)

Fig. 7 Image conversion corresponds with Fig. 5(b)

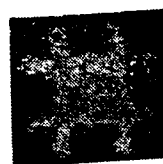
(a) white light image (input); (b) red or green image (output)



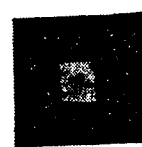
Fig. 8 Image conversion from green image (514.5) to red image (632.8 nm) corresponds with Fig. 5(a)



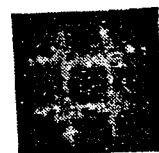
(a)



(b)



(c)



(d)

Fig. 9 Parallel image subtraction between coherent and incoherent images
 (a) the diagram of image subtraction by FWM and white writing; (b) coherent image for I_1 path inputting; (c) incoherent image for white light image inputting; (d) the result output of subtraction between (b) and (c)

In summary, such spatial light modulator has a simple structure and it can be reused; it responds quickly, makes a real-time operation, and furthermore without affecting the crystal itself, it has an advantage to be reused in the studies of various functions, such as nonlinear optics, and real-time holography, etc. Thus it adds a new important meaning to the development of photo-refractive crystals for the application research in spatial light modulators and optical computation.

A part of the experimental crystals was provided by Prof. Lianyen Zhi of Shanghai Institute of Silicon Oxide Salts; Comrade Lixin Yao of Beijing Institute of Technology took part in some section of the experimental work; Comrades Xifen Zhu, Yuhu Kung and Li Yao of Xian Optical Manufacturers provided a lot of assistance, and thus, thanks is due to all of them.

Reference

- [1] D. Casasent; *Opt. Engng*, 1978, 17, No. 4 (Jul/Aug), 307.
- [2] *Spatcal Light Modulations & Applications* 1988.
- [3] R. A. Sprague, P. Nisenson; *Opt. Engng*, 1978, 17, No. 4 (Jul/Aug). 256.
- [4] Y. Shi, D. Psaltis *et al.*; *Appl. Opt.*, 1983, 22, No. 23 (Dec), 3665.
- [5] Scapham, R. W. Eason *et al.*; *Opt. Commun*, 1990, 74, No. 5, 290.
- [6] Li Yulin, Zhao Mingjun; *Proc. SPIE*, 1990, Vol. 1358
- [7] W. J. Burke, D. L. Staebler *et al.*; *Opt. Engng*, 1978, 17, No. 4 (Jul/Aug). 308.

DISTRIBUTION LIST

DISTRIBUTION DIRECT TO RECIPIENT

<u>ORGANIZATION</u>	<u>MICROFICHE</u>
B085 DIA/RTS-2FI	1
C509 BALLOC509 BALLISTIC RES LAB	1
C510 R&T LABS/AVEADCOM	1
C513 ARRADCOM	1
C535 AVRADCOM/TSARCOM	1
C539 TRASANA	1
Q592 FSTC	4
Q619 MSIC REDSTONE	1
Q008 NTIC	1
Q043 AFMIC-IS	1
E051 HQ USAF/INET	1
E404 AEDC/DOF	1
E408 AFWL	1
E410 AFDIC/IN	1
E429 SD/IND	1
P005 DOE/ISA/DDI	1
P050 CIA/OCR/ADD/SD	2
1051 AFIT/LDE	1
PO90 NSA/CDB	1
2206 FSL	1

Microfiche Nbr: FTD95C000113
NAIC-ID(RS) T-0396-94